Review

Gold Nanoparticle Based Colorimetric Biosensing for Food Safety

Sang-Hyun Park and Youngsang You *

Posted Date: 30 November 2023

doi: 10.20944/preprints202311.1963.v1

Keywords: visible-signaling biosensor; localized surface plasmon resonance (LSPR); food quality; food safety; nanotechnology

Review

Gold Nanoparticle Based Colorimetric Biosensing for Food Safety

Sang-Hyun Park [1] and Youngsang You [2,*]

[1] Department of Food Science and Technology, Kongju National University, Yesan, Chungnam, 32439, Republic of Korea
[2] Department of Food Engineering, Dankook University, Cheonan, Chungnam 31116, Republic of Korea
* Correspondence: ysyou7@dankook.ac.kr

Abstract: Ensuring safe, high-quality food is an ongoing priority, yet consumers face heightened risk from foodborne pathogens due to extended supply chains and climate change in food industry. Nanomaterial-based assays are popular and have recently been developed to ensure food safety and high quality. This review discusses strategies for using nanomaterials in colorimetric biosensors. Localized surface plasmon resonance (LSPR) biosensors are commonly utilized for colorimetric biosensing. Several emerging technologies aimed at simple and rapid immunoassays for onsite applications have been introduced in the food industry. In the foreseeable future, field-friendly colorimetric biosensors could be adopted in food monitoring systems. The onsite and real-time detection of possible contaminants and biological substances in food and water is essential to ensure human health safety.

Keywords: visible-signaling biosensor; localized surface plasmon resonance (LSPR); food quality; food safety; nanotechnology

1. Introduction

Nutritional components, including carbohydrates, proteins, and lipids, are ingested to supply a variety of essential nutrients to the human body. Currently, governments place significant emphasis on upholding food quality and safety standards to foster human well-being and promote sustainability. The food industry, for instance, requires a novel, efficient, and user-friendly inspection method as an alternative to the current, time-consuming, costly, and cumbersome machinery. Surveillance of foodborne outbreaks plays a crucial role in the food industry due to the expanding scope of food distribution. The security and safety of distributed food hinge on the food producers' capacity to recognize, detect, and track foodborne pathogens [1]. Pathogens transmitted through food and water can lead to a spectrum of infections, with outcomes spanning from mild fever to fatal consequences [2–4]. Food regulatory agencies and manufacturers have diligently adopted numerous initiatives to reduce the risks associated with contamination by foodborne pathogens. These include the implementation of food cold chain systems and the adoption of hazard analysis and critical control point programs [5]. Nonetheless, the food industry still grapples with the challenge of curbing the incidence of foodborne disease outbreaks. Given the globalization of food supply chains, these outbreaks can occur simultaneously on a global scale due to the intricate food distribution systems in place. Consequently, there is a constant potential for escalating health and economic risks [6]. With conventional methods such as colony counting, the enzyme-linked immunosorbent assay (ELISA), and PCR, the onsite and rapid detection of foodborne pathogens are difficult to analyze. The prompt and precise identification of these pathogens is pivotal in preventing the dissemination of foodborne diseases.

Traditionally, pathogens were identified through colony counting and PCR, but these methods have inherent limitations due to their time-consuming, labor-intensive, lab-based, and costly nature [7,8]. The drawbacks of traditional detection techniques have spurred the innovation of biosensors

 doi:10.20944/preprints202311.1963.v1

designed to achieve swifter and more sensitive pathogen detection. Biosensors, as a cutting-edge analytical approach, are extensively employed for the analysis of food constituents. They typically consist of two primary elements: (1) a bioligand system responsible for recognizing and capturing the target, and (2) a signal transducer that converts biological information into a measurable signal [9,10]. These sensor varieties have experienced rapid development as substitutes for traditional analytical techniques, providing swift, highly selective, user-friendly, and cost-effective detection options [11]. Out of the many detection techniques available, biosensors, born from the fusion of molecular biology and material technology, hold great promise due to their remarkable reactivity, sensitivity, and selectivity [12,13]. Hence, immunosensors based on nanomaterials are gaining prominence in the realm of point-of-care testing, thanks to their exceptional attributes. Numerous biosensors have demonstrated remarkable sensitivity, including the capability to detect single-cell [14]. The main challenges in foodborne pathogen detection revolve around developing cost-effective and straightforward identification techniques that can detect multiple pathogens, exhibit specificity in distinguishing between various bacteria, and demonstrate sensitivity to detect bacteria in food samples without the need for pre-enrichment [15–17].

The integration of nanotechnology can enhance immunoassays, as nanoparticles possess distinctive physical, chemical, and optical characteristics that set them apart from their bulk counterparts. [18–21]. Notably, gold nanoparticles (AuNPs) have attracted considerable interest for their application in optical biosensors, primarily due to their optical properties, which are dependent on their size and aggregation [22]. This relationship has been harnessed to create AuNPs with diverse colors, sizes, and shapes. AuNPs have found utility in the detection of nucleic acids, proteins, and entire pathogenic cells. The functionalization of AuNPs with small molecules, proteins, or nucleic acids offers a wide array of applications [23–27].

This review provides an overview of diverse approaches to pathogen detection in food and drinking water. These findings serve as a foundation for enhancing food security in the face of potential infectious diseases. Section 1 outlines the fundamentals of the immunoassay method, while Section 2 delves into visible light biosensing for food safety, encompassing pathogens, pesticides, and toxins.

2. Localized surface plasmon resonance principles of the AuNP

Of the many visible-signal biosensors, specific surface plasmon resonance (SPR) biosensors offer sensitive, real-time, rapid, and label-free detection capabilities [28,29]. SPR produces an optical signal when the valence electronics oscillate and resonate in a solid metal generated by incident light [30,31]. The optical properties of metallic nanoparticles (MNPs) vary significantly based on their morphologies and sizes. In other words, the visible characteristics of MNPs are intricately connected to their SPR attributes. As shown in Figure 1a and b, when the surface plasmon is confined within an MNP that is smaller than the wavelength of the incoming light, the free electrons in the MNP collectively oscillate, a phenomenon known as localized surface plasmon (LSP) [32,33]. Subsequently, as they couple with incident photons of comparable frequencies, the free electron cloud initiates a synchronized oscillation in relation to the positively charged ions in the lattice, leading to the accumulation of polarization charges on the MNP's surface. This buildup of polarization charges, in turn, generates a Coulomb field that functions as a restoring force, propelling the electrons in the opposite direction and giving rise to the resonance effect (Figure 1a) [34,35]. As a result, localized surface plasmon resonance (LSPR) yields two primary outcomes: 1) a substantial enhancement of the electromagnetic field produced by nanoparticles, peaking at the surface but diminishing rapidly over a short distance, and 2) the optical extinction of MNPs at the resonance frequency, allowing for detection using conventional UV-Vis spectroscopy or other far-field scattering techniques (Figure 1b) [35,36]. The treatment of LSPR calculations and explanations can be found in the literature [37,38]. LSPR biosensors have attracted significant attention, offering several advantages, including reduced detection location limitation and high flexibility [39,40].

Specifically, gold nanoparticles (AuNPs) possess distinctive optical characteristics that make them extensively applicable in the detection of food- and water-borne pathogens using LSPR [41].

Preprints (www.preprints.org) | NOT PEER-REVIEWED | Posted: 30 November 2023 doi:10.20944/preprints202311.1963.v1

The color of the AuNP solution can be altered by modifying its morphology, including aspects like size and shape, as illustrated in Figure 1c and d [42]. Figures 1e, f, and g depict spherical AuNPs ranging from 5 to 50 nm, each exhibiting distinct absorbance peaks between 515 and 545 nm, along with their respective distributions [43]. Altering the shape of the AuNPs can also lead to changes in their SPR properties. Gold nanorods (AuNRs) display dual absorbance peaks—one associated with the transverse band and the other linked to the longitudinal band in the infrared range. The longitudinal band, especially when employed in immunoassays, proves to be more responsive [44]. This shift in absorbance is often adequate to induce a visible color change, rendering the technique well-suited for straightforward and onsite detection [45]. As the size and aggregation of AuNPs increase, there is a noticeable red shift in the peak absorbance, imparting a stable AuNP solution with a red color. In contrast, the aggregated state of AuNPs imparts a purple color (Figure 2a). This color alteration is readily perceivable to the unaided eye.

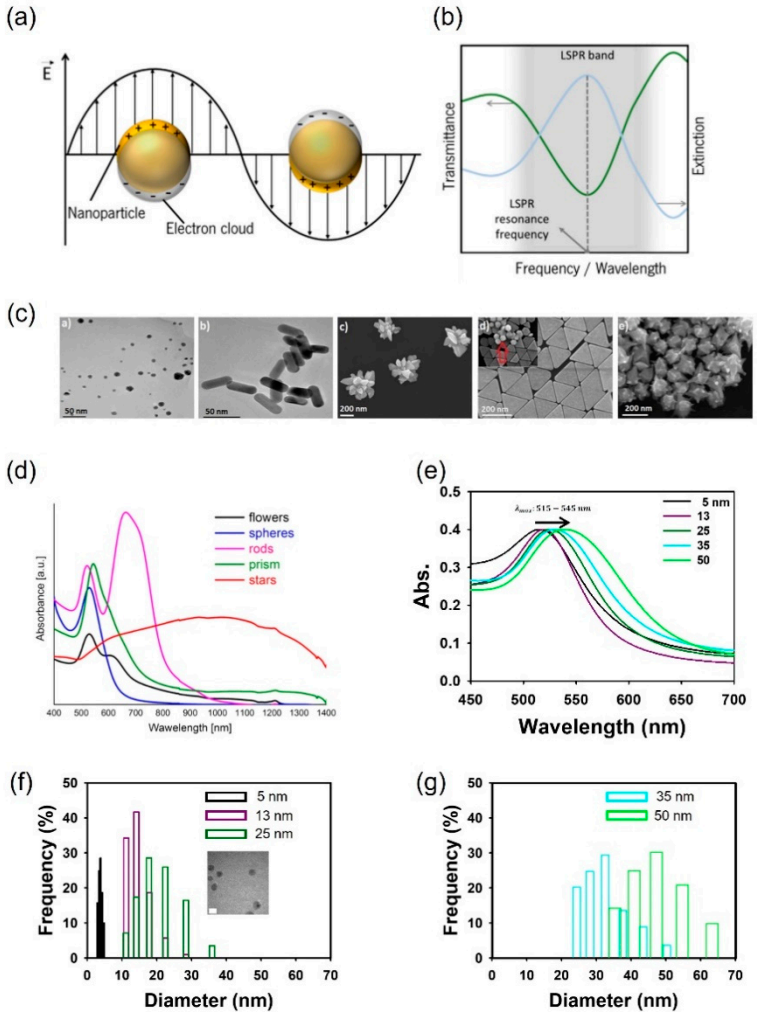

Figure 1. Schematics of localized surface plasmons of metal sphere (a). Schematics of a typical LSPR band, measured in transmittance mode, and extinction spectrum (b). TEM images of gold nanoparticles showed (sphere, nanorods, nanoflowers, nanoprism, and nanostars) (c). UV-Vis absorption spectra of gold nanoparticles with different shapes (d). Change in absorption spectra of five spherical gold nanoparticles in the range from 5-50 nm (e) and distribution of gold nanoparticles of diameters 5−25 nm (f) and 35 and 50 nm (g) synthesized by the citrate reduction of $HAuCl_4$. Figure adapted from Ref. [35,42].

Preprints (www.preprints.org) | NOT PEER-REVIEWED | Posted: 30 November 2023 doi:10.20944/preprints202311.1963.v1

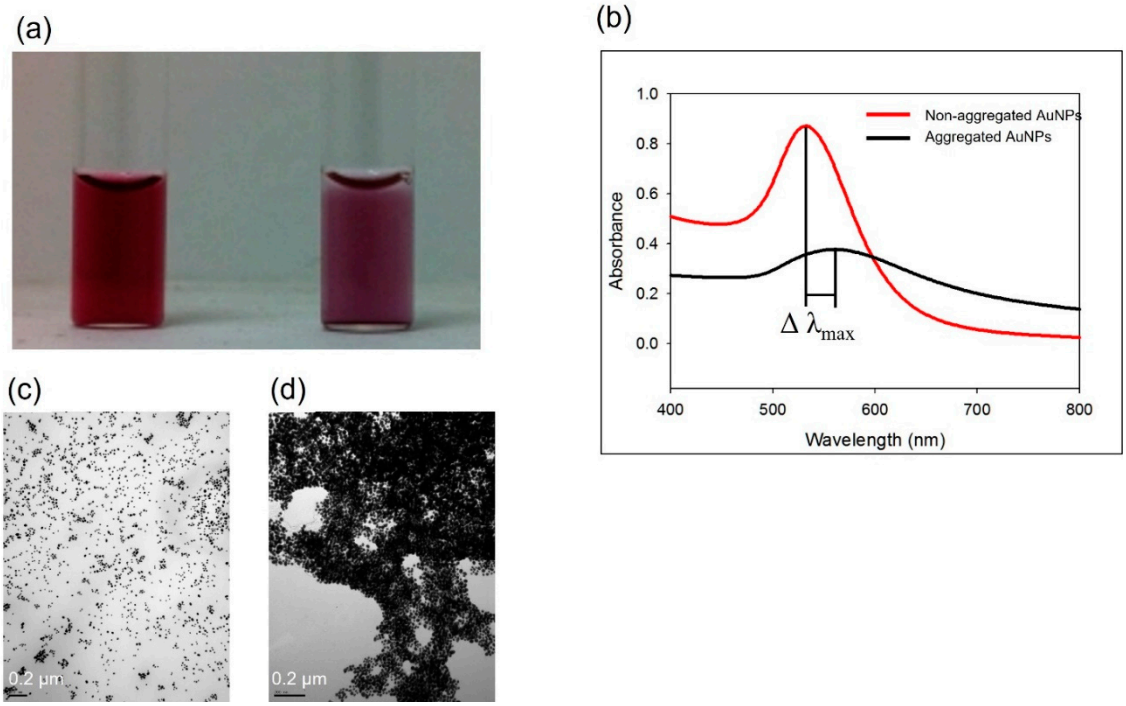

Figure 2. Color of non-aggregated (left) and aggregated (right) AuNPs (a). UV-Vis absorption spectra of aqueous solutions of AuNPs with 13 nm of diameter for non-aggregated (red) and aggregated (black) AuNPs (b). TEM images of non-aggregated AuNPs (c) and aggregated AuNPs (d).

3. Visible-signal strategies for ensuring food and agriculture product safety

3.1. Non-functionalized AuNPs for pathogen detection

Citrate is commonly used to stabilize AuNPs, with citrate-capped AuNPs carrying a negative charge, while cetyltrimethylammonium bromide (CTAB)-capped AuNPs, especially AuNRs, are positively charged. This technique allows for detection without the need for specific functionalization. Many studies have concentrated on the color transition of AuNPs from red to purple, primarily due to their electrostatic aggregation. Wang *et al*. [46] reported that *Vibrio parahaemolyticus* (*V. parahaemolyticus*), which is usually found in contaminated seafood, can be detected based on thiolated phage nanobody induced aggregation of AuNPs. In the presence of V. *parahaemolyticus* in the sample, the thiol groups in the phage did not trigger the aggregation of AuNPs. Nevertheless, the thiol group could induce AuNPs' aggregation when the thiolated phage nanobody was part of a sample lacking the target Vibrio. This method can achieve visual detection within 100 min as low as 10^3 CFU·mL^{-1} (Figure 3a and b) [46]. Bu *et al*. (2019) reported that *Salmonella* Enteritidis (*S.* Enteritidis) and *E. coli* O157 were detected by changing the surface charge of AuNPs. The negatively charged AuNPs were converted into positively charged surfaces using cysteamine and CTAB. The pathogens *S.* Enteritidis and *E. coli* O157 were captured by positively charged AuNPs, and the complex interacted with each bacterial antibody using a lateral flow strip (Figure 3c–e) [47]. Therefore, the aggregation of AuNPs occurred at the test line. Pathogens can be detected from 10^3 to 10^8 CFU·mL^{-1} by the naked eye. Guo *et al*. (2021) reported a highly sensitive detection method using a bacteria-imprinted polymer and fluorescent and label-free AuNPs within 135 min. Using fluorescence resonance energy transfer, this system achieved highly sensitive detection. In addition, the working range of this method is wide from 10 to 10^7 CFU·mL^{-1} of *staphylococcus aureus* (*S. aureus*) under optimum conditions [48].

Preprints (www.preprints.org) | NOT PEER-REVIEWED | Posted: 30 November 2023 doi:10.20944/preprints202311.1963.v1

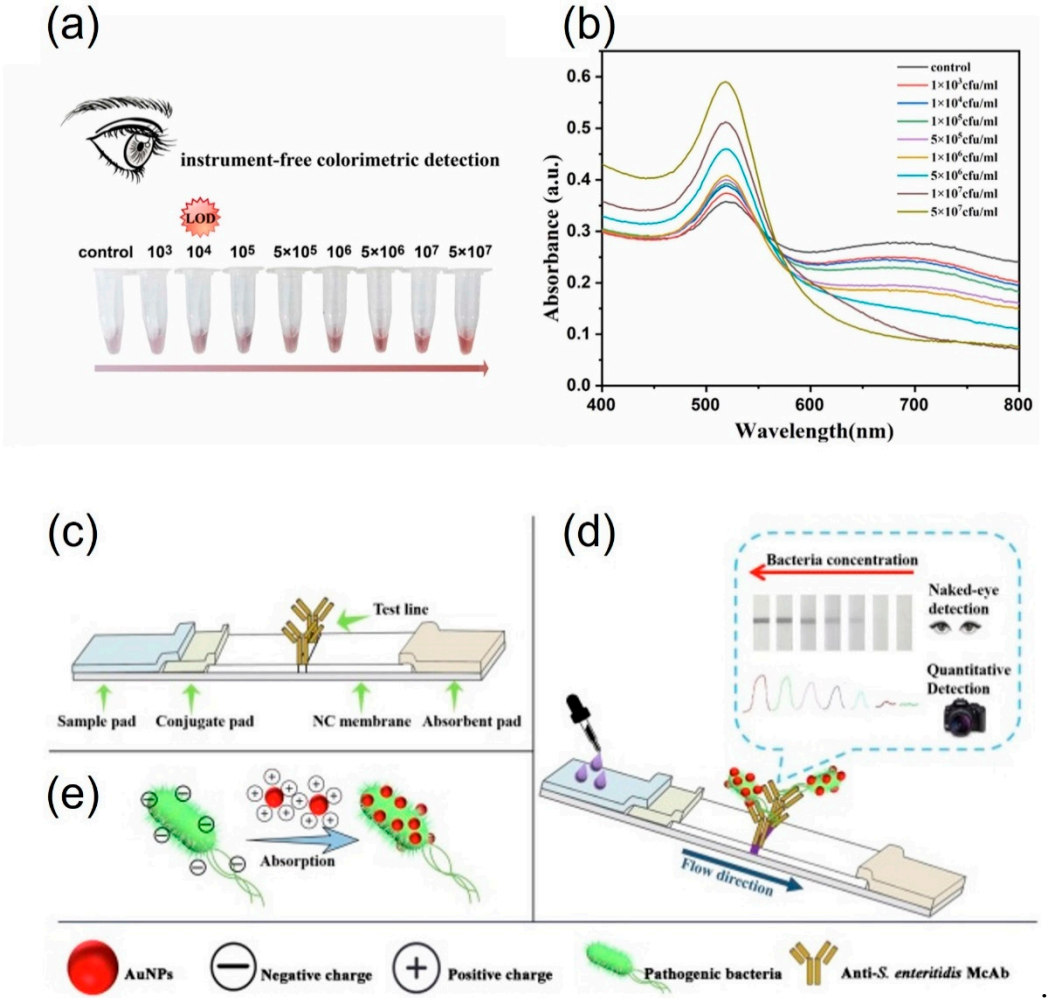

Figure 3. Detection of *V. parahaemolyticus* by the one-step colorimetric immunosensor with (a) naked eye and (b) UV–vis spectrometry. Schematic illustration of (c) the structure of the test strip (d), combining AuNPs with *S. enteritidis* (e), AuNPs and *S. enteritidis* flow from conjugate pad to absorbent pad, the appearance of the color of the *T*-line, and the principle of quantitative detection strategy of *S. enteritidis* using camera as readout. Figure adapted from Ref. [46,47].

Without the need for nucleic acid amplification, it is advantageous to reduce analysis time and avoid the use of specialized instruments. The use of non-functionalized AuNPs simplifies biosensing assays that produce colorimetric signals. The most crucial limitation of this method is the variety of interferons in the environment, which can cause the nonspecific aggregation of AuNPs and, therefore, produce false signals. The research using non-functionalized AuNPs for the detection of pathogens is summarized in Table 1.

Table 1. Summary of alternative food safety detection methods.

Types	Pathogens	Analysis time	Detection limit	Working range	Sample type	Ref.
Non-functionalized AuNPs	*E. coli* and *B. cereus*	~1 h	~10^8 CFU·mL^{-1}	ND[a]	Culture	[55]
	E. coli O157:H7 and *S. enterica*	20 min	10^5 CFU·mL^{-1}	10^5-10^8 CFU/mL	Culture	[56]

Preprints (www.preprints.org) | NOT PEER-REVIEWED | Posted: 30 November 2023 doi:10.20944/preprints202311.1963.v1

	S. aureus, *Achromobacter xylosoxidans*, *Delftia acidovorans*, and *Stenophomonas maltophilia*	~ 5 min	~1.5×10^{6} CFU·mL^{-1}	ND[a]	Culture	[57]
	Hepatitis C virus	~30 min	2.5 copies·μL^{-1} RNA	~2.5-100 copies·μL^{-1}	Serum	[58]
	Enterobacter cloacae	~35 min	16 fmol/mL of P99 β-lactamase	15-80 fmol·mL^{-1}	β-lactamase	[59]
	Vibrio parahaemolyticus	100 min	10^{3} cfu·mL^{-1}	10^{3}-10^{7} CFU·mL^{-1}	Spiked shrimp	[46]
	Salmonella enteritidis	n.d.[a]	10^{3} cfu·mL^{-1}	10^{3}-10^{8} CFU·mL^{-1}	Spiked lettuce and pork	[47,48]
	Staphylococcus aureus	135 min	10^{2} cfu·mL^{-1}	10^{2}-10^{4} CFU·mL^{-1}	Spiked pork	[48]
Protein functionalized AuNPs	*Staphylococcus aureus*	40 min	1.5×10^{7} CFU·mL^{-1} (milk) 1.5×10^{5} CFU·mL^{-1} (PBS)	1.5×10^{7}-1.5×10^{8} CFU·mL^{-1}	Spiked milk	[49]
	Pseudomonas aeruginosa	~ 3 min	5×10^{2} CFU·mL^{-1}	1.5×10^{5}-1.5×10^{8} CFU·mL^{-1}	ND[a]	[60]

Table 1. (continued).

Types	Pathogens	Analysis time	Detection limit	Working range	Sample type	Ref.
Protein functionalized AuNPs	*C. jejuni*	Overnight	10^{6} CFU·mL^{-1}	10^{6}-10^{9} CFU·mL^{-1}	Culture	[61]
	G. lambliacysts	ND[a]	1×10^{3} cells·mL^{-1}	10^{3}-10^{4} cells·mL^{-1}	Culture	[62]
	S. enterica serovar	< 5min	10^{3} CFU·mL^{-1}	10^{3}- 10^{4} CFU·mL^{-1}	Culture	[60]
	E. coli O157:H7	20 min	10^{3} cfu/mL 10^{0} cfu·mL^{-1} (with smartphone)	10^{3} to 10^{7} cfu·mL^{-1}	River and tap water	[50]
	Francisella tularensis	20 min	10^{3} cfu·mL^{-1}	10^{3} to 10^{9} cfu·mL^{-1}	Natural and tap water	[51]
	S. aureus	~2 h	50 CFU·mL^{-1}	5×10^{2} – 5×10^{6} CFU·mL^{-1}	Spiked milk, urine, lung fluid	[53]
Small molecule functionalized AuNPs	*E. coli* 055:B5 LPS	~5 min	330 fmol/mL lipopolysaccharides	5-90 pmol·mL^{-1}	ND[a]	[63]
	E. coli O157:H7	< 40 min	7 CFU·mL^{-1}	7-6×10^{6} CFU·mL^{-1}	Culture	[64,65]
	Influenza B/Victoria and Influenza B/Yamagata	~10 min	0.15 vol% dilution of Hemagglutination assay titer 512 virus	0.15 -1.25 vol%	Culture	[66]

 doi:10.20944/preprints202311.1963.v1

	E. coli XL1	~10 min	10^2 CFU·mL^{-1} (solution) 10^4 CFU/mL (test strip)	10^2 – 10^7 CFU·mL^{-1} (solution) 10^4 – 10^8 CFU·mL^{-1} (test strip)	Culture	[67]

[a]: Not detected.

3.2. Protein-functionalized AuNPs for pathogen detection

AuNPs can be readily modified with antibodies to facilitate their selective binding to target antigens present on bacterial surfaces. This technique induces the clustering of AuNPs in the vicinity of the target bacteria's surface due to interactions between antibodies and antigens. An alternative approach involves using the clustering of AuNPs that have been modified with antibodies as a labeling technique to enhance signals by promoting the growth of gold around the original seed particles. As a result, AuNPs have been employed in immune complex (IC) systems as a substitute for ELISA.

A limited level of AuNP aggregation yields an inadequate signal strength, requiring improvement in the signal amplification phase to enhance the signal. Consequently, signal enhancement can be accomplished by introducing a higher concentration of target bacteria into the system. The filtration method can be combined with magnetic nanoparticles for use with complicated samples. This method has been previously used to detect *S. aureus* in milk. First, bovine serum albumin-functionalized magnetic nanoparticles were synthesized and coated with anti-*S. aureus* antibodies. This complex system of magnetic nanoparticles was then added to the target bacteria-contaminated samples. Second, after incubation time, the mixture was filtered to the target 0.8 μm cellulose acetate membrane. Filtration can separate bacteria attached to magnetic nanoparticles from unbound magnetic nanoparticles because small unbound magnetic nanoparticles can pass through the filtration membrane. Finally, the gold growth solution produced a color change on the surface of the filter [49].

Fluorescent gold nanoclusters (AuNCs) and AuNPs were utilized as rapid, simple, and cost-effective detection systems. In the first step, fluorescent AuNCs were drop-cast onto a fiberglass membrane. *E. coli* O157:H7 antibody conjugated AuNPs were then loaded into microtubes with fluorescent AuNCs. For detection, *E. coli* O157:H7 samples were placed in microtubes. After a 20 min incubation step, visible sensing was evaluated through Förster resonance energy transfer. Using this method, visible sensing can be achieved from 10^3 to 10^7 CFU·mL^{-1}. Moreover, color recognition can also be achieved using the image sensor of a smartphone. The detection range of a smartphone is from 0 to 10^7 CFU·mL^{-1} [50]. The detection method for whole cells of *Francisella tularensis* (*F. tularensis*) was reported by Byzova *et al.* (2022) [51]. *F. tularensis* could be recognized by monoclonal antibodies in both natural and tap water samples. For visible-signal production, AuNPs of different sizes ranging from 26.6 to 41.8 nm were utilized. The visible detection system consisted of an *F. tularensis* monoclonal antibody and AuNPs. The antibody conjugated AuNPs could recognize 0–10^7 CFU·mL^{-1} of *F. tularensis* and produce signals within 20 min (Figure 4a, b, and d) [50]. This system can detect the presence of *F. tularensis* whole cells at concentrations as low as 3×10^3 CFU·mL^{-1} using a color change (Figure 4c) [50]. Moreover, *F. tularensis* lipopolysaccharide was also detected using the same system.

Antibody-functionalized AuNPs can identify pathogens by leveraging their distinct optical characteristics, reducing the need for extensive sample preparation and signal generation. In comparison to ELISA, the detection of pathogens in samples was achieved using paper substrates immobilized with functionalized AuNPs, such as in immune complexes (ICs). This approach is less complex compared to the conventional ELISA, making it easily transportable and demanding only minimal training. Protein-functionalized AuNP methods have certain limitations: the assay still requires certain laboratory instruments for concentrating the sample, which is frequently only

Preprints (www.preprints.org) | NOT PEER-REVIEWED | Posted: 30 November 2023 doi:10.20944/preprints202311.1963.v1

available in the laboratory and requires technical expertise for testing. The methods for pathogen detection using protein-functionalized AuNPs are summarized in Table 1.

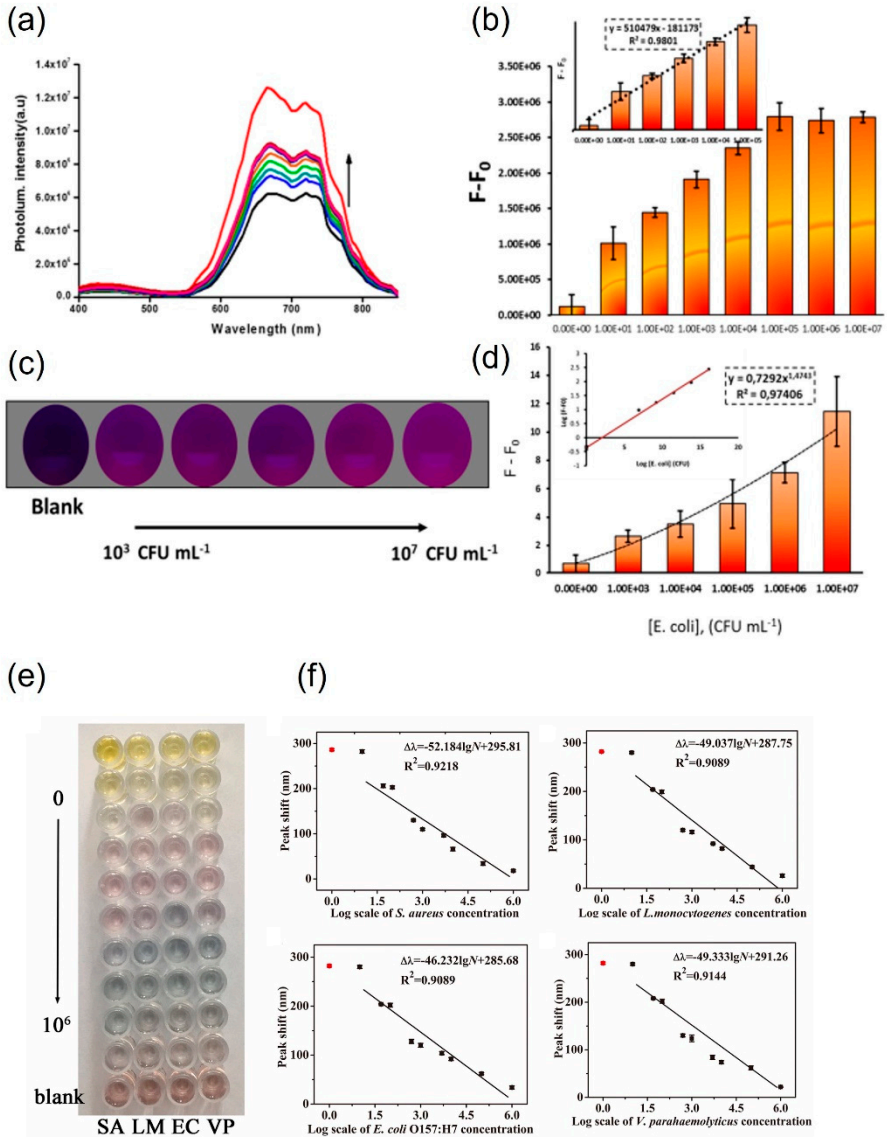

Figure 4. Quantification of *E. coli* O157:H7 using a developed biosensor. (a) Fluorescence spectrum of AuNCs/Ab-AuNPs upon addition of different concentrations of *E. coli* from 0 to 10^7 CFU·mL^{-1}. (b) Calibration curve of the assay using a fluorimeter. (F and F_0 correspond to the fluorescence intensities of the AuNCs/AuNPs system in the presence and absence of *E. coli* , respectively). (c) Typical images of the AuNCs/AbAuNPs system in the presence of various concentrations of E. coli in the range of 0–10^7 cfu·mL^{-1} (0, 10^3, 10^4, 10^5, and 10^6 cfu·mL^{-1} from left to right) captured using a smartphone camera under 365 nm UV light irradiation. (d) Calibration curve resulting from processing images in the smartphone. Error bars represent the standard deviation (n = 3). Inset: linear behavior of a power function. Photograph (e) and calibration curves (f, peak shift vs the logarithm of bacteria concentration) of the proposed multicolorimetric assay detecing foodborne pathogenic bacteria at various concentrations (0, 1.0×10, 5.0×10, 1.0×10^2, 5.0×10^2, 1.0×10^3, 5.0×10^3, 1.0×10^4, 1.0×10^5, and 1.0×10^6 CFU·mL^{-1}). Figure adapted from Ref. [50,52].

3.3. Small-molecule-functionalized AuNPs for pathogen detection

AuNPs modified with small molecules are capable of identifying food- and water-borne pathogens through electrostatic, covalent, or receptor-mediated interactions. In such instances, these AuNPs functionalized with small molecules have the ability to cluster around the specified pathogen.

 doi:10.20944/preprints202311.1963.v1

Figure 4e and f illustrate the implementation of a multi-detection strategy incorporating nanocomposites [52]. The bacterial probe utilized was the Aptramer-Fe_3O_4/MnO_2 nanocomposite. In the initial stage, the nanocomposite was engaged with the target bacteria, followed by the mixing of gold nanorods with tetramethylbenzidine (oxTMB) for the detection of *E. coli* O157:H7, *S. aureus*, *Listeria monocytogenes*, and *V. parahaemolyticus*. The oxidative activity of the Aptramer-Fe_3O_4/MnO_2 nanocomposite diminishes, leading to the conversion of oxTMB to AuNRs and inducing a polychromatic alteration. AuNRs act as peroxidase mimics, facilitating the oxidation of 3,3′,5,5′-TMB by hydrogen peroxide. Upon combining functionalized AuNRs with the target bacteria in the sample, the functionalized gold nanoparticles aggregate on the surface of the pathogen. Observable color changes are discernible by the naked eye within 40 min [17]. In another study, 13 nm AuNPs functionalized with dithiodialiphatic acid-3aminophenylboronic acid were employed for the detection of *S. aureus*. In this approach, the functionalized AuNPs interact with *S. aureus* and are subsequently isolated through centrifugation. The separated pathogens appear red because of the characteristics of the 13 nm AuNPs [53].

In an alternative approach, AuNPs functionalized with sialic acid were employed for the detection of both bacteria and viruses. In the case of influenza viruses, hemagglutinin, present on their surface, is recognized as sialic acid in the host cell during the infection process. The detection of target viruses is achieved through hemagglutinin, as it facilitates the aggregation of sialic acid-functionalized AuNPs. In this approach, a mixture of trivalent α2,6-thio-linked sialic acid-functionalized AuNPs and the influenza virus results in a noticeable color change [54].

Utilizing small-molecule-functionalized AuNPs facilitates swift and highly sensitive detection. Furthermore, small molecules are more cost-effective compared to other substances like proteins, antibodies, and nucleic acids, making the overall cost of this sensor lower than alternative sensing methods. Nevertheless, small-molecule-functionalized AuNPs lack specificity for target pathogens, as some pathogens may produce identical enzymes. Consequently, this approach could yield a false positive response when closely related pathogens are present in a sample. The detection methods employing small-molecule-functionalized AuNPs are outlined in Table 1.

To summarize, both functionalized and non-functionalized AuNPs have been employed in colorimetric pathogen detection, targeting surface proteins and whole cells. The objective of this immunoassay is to create methods or devices capable of on-site detection, offering a straightforward visual output. While functionalized AuNPs have contributed to the advancement of simple and rapid immunoassays, these biosensors face challenges in sensitivity when target pathogens are present in complex matrices.

4. Conclusions and Prospects

Ensuring the quality and safety of food is crucial for both national governments and food producers, as it directly impacts human health. The effective identification of chemical and biochemical targets in food plays a key role in accurately predicting and diagnosing the health status of food products. In the last few decades, visible-signal biosensors, especially those based on LSPR, have found extensive application in the real-time and on-site detection of food analytes. The sensitivity of LSPR biosensors has been further heightened through the utilization of functional metal nanoparticles with distinctive optical properties, facilitated by advances in nanotechnology. Within the realm of MNPs, AuNPs and AgNPs stand out as the most widely accepted for achieving highly sensitive analyte determination due to their stability and ease of preparation. Consequently, a majority of these products are presently available to ensure the maintenance of quality and safety in food and agricultural products.

Advancements in recent times have endowed optical biosensors with increased advantages for the analysis of food quality and safety. Nonetheless, there are still several challenges that researchers need to tackle.

The primary challenge confronting researchers in food analysis is achieving ultrasensitive detection. While employing an LSPR optical biosensor for directly determining a single atomic or molecular analyte may not be practical, there is a crucial need for advancements in distinguishing

analytes of smaller sizes. Moreover, ensuring the stability and reproducibility (selectivity) of LSPR biosensors poses significant challenges. As outlined in this review, numerous factors contribute to the LSPR peak shift. In this context, preserving the optical biosensor before analysis becomes a concern, especially for LSPR biosensors employing an aggregation mechanism. Finally, due to the diverse interferences present in complex solutions, it is imperative that the signal produced by the SPR biosensor remains consistent in both standard and complex solutions.

Acknowledgements: This work was supported in part by the National Research Foundation of Korea (NRF) grant (No.2021R1A1093642) from the Government of Korea Ministry of Science and ICT.

Conflicts of interest statement: Conflict of interest the authors declare no conflict.

References

1. Zhang, Y.; Simpson, R.B.; Sallade, L.E.; Sanchez, E.; Monahan, K.M.; Naumova, E.N. Evaluating Completeness of Foodborne Outbreak Reporting in the United States, 1998–2019. *Int J Environ Res Public Health* **2022**, *19*, 2898.
2. Aiyedun, S.O.; Onarinde, B.A.; Swainson, M.; Dixon, R.A. Foodborne Outbreaks of Microbial Infection from Fresh Produce in Europe and North America: A Systematic Review of Data from This Millennium. *Int J Food Sci Technol* **2021**, *56*, 2215–2223.
3. Collins, J.P.; Shah, H.J.; Weller, D.L.; Ray, L.C.; Smith, K.; McGuire, S.; Trevejo, R.T.; Jervis, R.H.; Vugia, D.J.; Rissman, T. Preliminary Incidence and Trends of Infections Caused by Pathogens Transmitted Commonly through Food—Foodborne Diseases Active Surveillance Network, 10 US Sites, 2016–2021. *Morbidity and Mortality Weekly Report* **2022**, *71*, 1260.
4. Helms, M.; Simonsen, J.; Mølbak, K. Foodborne Bacterial Infection and Hospitalization: A Registry-Based Study. *Clinical Infectious Diseases* **2006**, *42*, 498–506, doi:10.1086/499813.
5. Zeb, A.; Ayesha, R.; Gilani, S.A.; Shahbaz, M.; Imran, A.; El-Ghorab, A.; El-Massry, K.F.; Suleman, R.; Gondal, T.A.; Asif, M.; et al. Safety Assessment of Foods at Capital Hospital of Pakistan through the Hazard Analysis and Critical Control Point System. *J Food Prot* **2020**, *83*, 1387–1395, doi:https://doi.org/10.4315/0362-028X.JFP-18-602.
6. Lee, H.; Yoon, Y. Etiological Agents Implicated in Foodborne Illness World Wide. *Food Sci Anim Resour* **2021**, *41*, 1.
7. Nassarawa, S.S.; Luo, Z.; Lu, Y. Conventional and Emerging Techniques for Detection of Foodborne Pathogens in Horticulture Crops: A Leap to Food Safety. *Food Bioproc Tech* **2022**, *15*, 1248–1267.
8. Quintela, I.A.; Vasse, T.; Lin, C.-S.; Wu, V.C.H. Advances, Applications, and Limitations of Portable and Rapid Detection Technologies for Routinely Encountered Foodborne Pathogens. *Front Microbiol* **2022**, *13*, 1054782.
9. Gaudin, V. Advances in Biosensor Development for the Screening of Antibiotic Residues in Food Products of Animal Origin–A Comprehensive Review. *Biosens Bioelectron* **2017**, *90*, 363–377.
10. Verma, N.; Bhardwaj, A. Biosensor Technology for Pesticides—a Review. *Appl Biochem Biotechnol* **2015**, *175*, 3093–3119.
11. Goode, J.A.; Rushworth, J.V.H.; Millner, P.A. Biosensor Regeneration: A Review of Common Techniques and Outcomes. *Langmuir* **2015**, *31*, 6267–6276.
12. Kumar, N.; Kumari, M.; Arun, R.K. Development and Implementation of Portable Biosensors in Microfluidic Point-of-Care Devices for Pathogen Detection. In *Miniaturized Biosensing Devices: Fabrication and Applications*; Springer, 2022; pp. 99–122.
13. Xu, L.; Bai, X.; Bhunia, A.K. Current State of Development of Biosensors and Their Application in Foodborne Pathogen Detection. *J Food Prot* **2021**, *84*, 1213–1227.
14. Li, H.; Hsieh, K.; Wong, P.K.; Mach, K.E.; Liao, J.C.; Wang, T.-H. Single-Cell Pathogen Diagnostics for Combating Antibiotic Resistance. *Nature Reviews Methods Primers* **2023**, *3*, 6.
15. Azzouz, A.; Hejji, L.; Kim, K.-H.; Kukkar, D.; Souhail, B.; Bhardwaj, N.; Brown, R.J.C.; Zhang, W. Advances in Surface Plasmon Resonance–Based Biosensor Technologies for Cancer Biomarker Detection. *Biosens Bioelectron* **2022**, *197*, 113767.
16. Pissuwan, D.; Gazzana, C.; Mongkolsuk, S.; Cortie, M.B. Single and Multiple Detections of Foodborne Pathogens by Gold Nanoparticle Assays. *Wiley Interdiscip Rev Nanomed Nanobiotechnol* **2020**, *12*, e1584.

17. Zhang, H.; Yao, S.; Song, X.; Xu, K.; Wang, J.; Li, J.; Zhao, C.; Jin, M. One-Step Colorimetric Detection of Staphylococcus Aureus Based on Target-Induced Shielding against the Peroxidase Mimicking Activity of Aptamer-Functionalized Gold-Coated Iron Oxide Nanocomposites. *Talanta* **2021**, *232*, 122448, doi:https://doi.org/10.1016/j.talanta.2021.122448.
18. Evanoff Jr, D.D.; Chumanov, G. Synthesis and Optical Properties of Silver Nanoparticles and Arrays. *ChemPhysChem* **2005**, *6*, 1221–1231.
19. Kelly, K.L.; Coronado, E.; Zhao, L.L.; Schatz, G.C. The Optical Properties of Metal Nanoparticles: The Influence of Size, Shape, and Dielectric Environment. *J Phys Chem B* 2003, *107*, 668–677.
20. Shafiqa, A.R.; Abdul Aziz, A.; Mehrdel, B. Nanoparticle Optical Properties: Size Dependence of a Single Gold Spherical Nanoparticle. In Proceedings of the Journal of Physics: Conference Series; IOP Publishing, 2018; Vol. 1083, p. 012040.
21. Zhang, Y.; Wang, Y. Nonlinear Optical Properties of Metal Nanoparticles: A Review. *RSC Adv* **2017**, *7*, 45129–45144.
22. Rechberger, W.; Hohenau, A.; Leitner, A.; Krenn, J.R.; Lamprecht, B.; Aussenegg, F.R. Optical Properties of Two Interacting Gold Nanoparticles. *Opt Commun* **2003**, *220*, 137–141.
23. Goodman, C.M.; McCusker, C.D.; Yilmaz, T.; Rotello, V.M. Toxicity of Gold Nanoparticles Functionalized with Cationic and Anionic Side Chains. *Bioconjug Chem* **2004**, *15*, 897–900.
24. Kumar, A.; Ma, H.; Zhang, X.; Huang, K.; Jin, S.; Liu, J.; Wei, T.; Cao, W.; Zou, G.; Liang, X.-J. Gold Nanoparticles Functionalized with Therapeutic and Targeted Peptides for Cancer Treatment. *Biomaterials* **2012**, *33*, 1180–1189.
25. Thomas, K.G.; Kamat, P. V Chromophore-Functionalized Gold Nanoparticles. *Acc Chem Res* **2003**, *36*, 888–898.
26. Tiwari, P.M.; Vig, K.; Dennis, V.A.; Singh, S.R. Functionalized Gold Nanoparticles and Their Biomedical Applications. *Nanomaterials* **2011**, *1*, 31–63.
27. Zeng, S.; Yong, K.-T.; Roy, I.; Dinh, X.-Q.; Yu, X.; Luan, F. A Review on Functionalized Gold Nanoparticles for Biosensing Applications. *Plasmonics* **2011**, *6*, 491–506.
28. Scarano, S.; Mascini, M.; Turner, A.P.F.; Minunni, M. Surface Plasmon Resonance Imaging for Affinity-Based Biosensors. *Biosens Bioelectron* **2010**, *25*, 957–966.
29. Singh, P. SPR Biosensors: Historical Perspectives and Current Challenges. *Sens Actuators B Chem* **2016**, *229*, 110–130.
30. Liedberg, B.; Nylander, C.; Lundström, I. Biosensing with Surface Plasmon Resonance—How It All Started. *Biosens Bioelectron* **1995**, *10*, i–ix.
31. Nguyen, H.H.; Park, J.; Kang, S.; Kim, M. Surface Plasmon Resonance: A Versatile Technique for Biosensor Applications. *Sensors* **2015**, *15*, 10481–10510.
32. Hutter, E.; Fendler, J.H. Exploitation of Localized Surface Plasmon Resonance. *Advanced materials* **2004**, *16*, 1685–1706.
33. Unser, S.; Bruzas, I.; He, J.; Sagle, L. Localized Surface Plasmon Resonance Biosensing: Current Challenges and Approaches. *Sensors* **2015**, *15*, 15684–15716.
34. Cao, J.; Sun, T.; Grattan, K.T. V Gold Nanorod-Based Localized Surface Plasmon Resonance Biosensors: A Review. *Sens Actuators B Chem* **2014**, *195*, 332–351.
35. Rodrigues, M.S.; Borges, J.; Lopes, C.; Pereira, R.M.S.; Vasilevskiy, M.I.; Vaz, F. Gas Sensors Based on Localized Surface Plasmon Resonances: Synthesis of Oxide Films with Embedded Metal Nanoparticles, Theory and Simulation, and Sensitivity Enhancement Strategies. *Applied Sciences* **2021**, *11*, 5388.
36. Sherry, L.J.; Jin, R.; Mirkin, C.A.; Schatz, G.C.; Van Duyne, R.P. Localized Surface Plasmon Resonance Spectroscopy of Single Silver Triangular Nanoprisms. *Nano Lett* **2006**, *6*, 2060–2065.
37. Agrawal, A.; Cho, S.H.; Zandi, O.; Ghosh, S.; Johns, R.W.; Milliron, D.J. Localized Surface Plasmon Resonance in Semiconductor Nanocrystals. *Chem Rev* **2018**, *118*, 3121–3207.
38. Willets, K.A.; Van Duyne, R.P. Localized Surface Plasmon Resonance Spectroscopy and Sensing. *Annu. Rev. Phys. Chem.* **2007**, *58*, 267–297.
39. Haes, A.J.; Van Duyne, R.P. A Unified View of Propagating and Localized Surface Plasmon Resonance Biosensors. *Anal Bioanal Chem* **2004**, *379*, 920–930.
40. Yonzon, C.R.; Jeoung, E.; Zou, S.; Schatz, G.C.; Mrksich, M.; Van Duyne, R.P. A Comparative Analysis of Localized and Propagating Surface Plasmon Resonance Sensors: The Binding of Concanavalin A to a Monosaccharide Functionalized Self-Assembled Monolayer. *J Am Chem Soc* **2004**, *126*, 12669–12676.

41. Daniel, M.-C.; Astruc, D. Gold Nanoparticles: Assembly, Supramolecular Chemistry, Quantum-Size-Related Properties, and Applications toward Biology, Catalysis, and Nanotechnology. *Chem Rev* **2004**, *104*, 293–346.
42. Woźniak, A.; Malankowska, A.; Nowaczyk, G.; Grześkowiak, B.F.; Tuśnio, K.; Słomski, R.; Zaleska-Medynska, A.; Jurga, S. Size and Shape-Dependent Cytotoxicity Profile of Gold Nanoparticles for Biomedical Applications. *J Mater Sci Mater Med* **2017**, *28*, 1–11.
43. Ghosh, D.; Chattopadhyay, N. Gold and Silver Nanoparticles Based Superquenching of Fluorescence: A Review. *J Lumin* **2015**, *160*, 223–232.
44. Wang, C.; Chen, Y.; Wang, T.; Ma, Z.; Su, Z. Biorecognition-Driven Self-Assembly of Gold Nanorods: A Rapid and Sensitive Approach toward Antibody Sensing. *Chemistry of Materials* **2007**, *19*, 5809–5811, doi:10.1021/cm0700899.
45. Sanromán-Iglesias, M.; Zhang, K.A.I.; Chuvilin, A.; Lawrie, C.H.; Grzelczak, M.; Liz-Marzán, L.M. Conjugated Polymers as Molecular Gates for Light-Controlled Release of Gold Nanoparticles. *ACS Appl Mater Interfaces* **2015**, *7*, 15692–15695.
46. Wang, P.; Yu, G.; Wei, J.; Liao, X.; Zhang, Y.; Ren, Y.; Zhang, C.; Wang, Y.; Zhang, D.; Wang, J.; et al. A Single Thiolated-Phage Displayed Nanobody-Based Biosensor for Label-Free Detection of Foodborne Pathogen. *J Hazard Mater* **2023**, *443*, 130157, doi:https://doi.org/10.1016/j.jhazmat.2022.130157.
47. Bu, T.; Jia, P.; Liu, J.; Liu, Y.; Sun, X.; Zhang, M.; Tian, Y.; Zhang, D.; Wang, J.; Wang, L. Diversely Positive-Charged Gold Nanoparticles Based Biosensor: A Label-Free and Sensitive Tool for Foodborne Pathogen Detection. *Food Chem X* **2019**, *3*, 100052, doi:https://doi.org/10.1016/j.fochx.2019.100052.
48. Guo, Y.; Li, J.; Song, X.; Xu, K.; Wang, J.; Zhao, C. Label-Free Detection of Staphylococcus Aureus Based on Bacteria-Imprinted Polymer and Turn-on Fluorescence Probes. *ACS Appl Bio Mater* **2021**, *4*, 420–427, doi:10.1021/acsabm.0c00897.
49. Sung, Y.J.; Suk, H.-J.; Sung, H.Y.; Li, T.; Poo, H.; Kim, M.-G. Novel Antibody/Gold Nanoparticle/Magnetic Nanoparticle Nanocomposites for Immunomagnetic Separation and Rapid Colorimetric Detection of Staphylococcus Aureus in Milk. *Biosens Bioelectron* **2013**, *43*, 432–439, doi:https://doi.org/10.1016/j.bios.2012.12.052.
50. Amin, N.; Torralba, A.S.; Álvarez-Diduk, R.; Afkhami, A.; Merkoçi, A. Lab in a Tube: Point-of-Care Detection of Escherichia Coli. *Anal Chem* **2020**, *92*, 4209–4216, doi:10.1021/acs.analchem.9b04369.
51. Byzova, N.A.; Zherdev, A. V; Gorbatov, A.A.; Shevyakov, A.G.; Biketov, S.F.; Dzantiev, B.B. Rapid Detection of Lipopolysaccharide and Whole Cells of Francisella Tularensis Based on Agglutination of Antibody-Coated Gold Nanoparticles and Colorimetric Registration. *Micromachines (Basel)* **2022**, *13*, 2194.
52. Zhang, H.; Liu, Y.; Yao, S.; Shang, M.; Zhao, C.; Li, J.; Wang, J. A Multicolor Sensing System for Simultaneous Detection of Four Foodborne Pathogenic Bacteria Based on Fe3O4/MnO2 Nanocomposites and the Etching of Gold Nanorods. *Food and Chemical Toxicology* **2021**, *149*, 112035.
53. Wang, J.; Gao, J.; Liu, D.; Han, D.; Wang, Z. Phenylboronic Acid Functionalized Gold Nanoparticles for Highly Sensitive Detection of Staphylococcus Aureus. *Nanoscale* **2012**, *4*, 451–454.
54. Marín, M.J.; Rashid, A.; Rejzek, M.; Fairhurst, S.A.; Wharton, S.A.; Martin, S.R.; McCauley, J.W.; Wileman, T.; Field, R.A.; Russell, D.A. Glyconanoparticles for the Plasmonic Detection and Discrimination between Human and Avian Influenza Virus. *Org Biomol Chem* **2013**, *11*, 7101–7107.
55. Jiang, T.; Liu, R.; Huang, X.; Feng, H.; Teo, W.; Xing, B. Colorimetric Screening of Bacterial Enzyme Activity and Inhibition Based on the Aggregation of Gold Nanoparticles. *Chemical communications* **2009**, 1972–1974.
56. Wu, W.; Li, M.; Wang, Y.; Ouyang, H.; Wang, L.; Li, C.; Cao, Y.; Meng, Q.; Lu, J. Aptasensors for Rapid Detection of Escherichia Coli O157:H7 and Salmonella Typhimurium. *Nanoscale Res Lett* **2012**, *7*, 658, doi:10.1186/1556-276X-7-658.
57. Verma, M.S.; Chen, P.Z.; Jones, L.; Gu, F.X. Branching and Size of CTAB-Coated Gold Nanostars Control the Colorimetric Detection of Bacteria. *RSC Adv* **2014**, *4*, 10660–10668.
58. Shawky, S.M.; Bald, D.; Azzazy, H.M.E. Direct Detection of Unamplified Hepatitis C Virus RNA Using Unmodified Gold Nanoparticles. *Clin Biochem* **2010**, *43*, 1163–1168, doi:https://doi.org/10.1016/j.clinbiochem.2010.07.001.
59. Liu, R.; Teo, W.; Tan, S.; Feng, H.; Padmanabhan, P.; Xing, B. Metallic Nanoparticles Bioassay for Enterobacter Cloacae P99 β-Lactamase Activity and Inhibitor Screening. *Analyst* **2010**, *135*, 1031–1036.

60. Pandey, S.K.; Suri, C.R.; Chaudhry, M.; Tiwari, R.P.; Rishi, P. A Gold Nanoparticles Based Immuno-Bioprobe for Detection of Vi Capsular Polysaccharide of Salmonella Enterica Serovar Typhi. *Mol Biosyst* **2012**, *8*, 1853–1860.
61. Cao, C.; Gontard, L.C.; Tram, T.; Ly, L.; Wolff, A.; Bang, D.D. Dual Enlargement of Gold Nanoparticles: From Mechanism to Scanometric Detection of Pathogenic Bacteria. *Small* **2011**, *7*, 1701–1708.
62. Li, X.X.; Cao, C.; Han, S.J.; Sim, S.J. Detection of Pathogen Based on the Catalytic Growth of Gold Nanocrystals. *Water Res* **2009**, *43*, 1425–1431, doi:https://doi.org/10.1016/j.watres.2008.12.024.
63. Sun, J.; Ge, J.; Liu, W.; Wang, X.; Fan, Z.; Zhao, W.; Zhang, H.; Wang, P.; Lee, S.-T. A Facile Assay for Direct Colorimetric Visualization of Lipopolysaccharides at Low Nanomolar Level. *Nano Res* **2012**, *5*, 486–493, doi:10.1007/s12274-012-0234-1.
64. Su, H.; Zhao, H.; Qiao, F.; Chen, L.; Duan, R.; Ai, S. Colorimetric Detection of Escherichia Coli O157:H7 Using Functionalized Au@Pt Nanoparticles as Peroxidase Mimetics. *Analyst* **2013**, *138*, 3026–3031, doi:10.1039/C3AN00026E.
65. Su, H.; Ma, Q.; Shang, K.; Liu, T.; Yin, H.; Ai, S. Gold Nanoparticles as Colorimetric Sensor: A Case Study on E. Coli O157:H7 as a Model for Gram-Negative Bacteria. *Sens Actuators B Chem* **2012**, *161*, 298–303, doi:https://doi.org/10.1016/j.snb.2011.10.035.
66. Lee, C.; Gaston, M.A.; Weiss, A.A.; Zhang, P. Colorimetric Viral Detection Based on Sialic Acid Stabilized Gold Nanoparticles. *Biosens Bioelectron* **2013**, *42*, 236–241, doi:10.1016/j.bios.2012.10.067.
67. Miranda, O.R.; Li, X.; Garcia-Gonzalez, L.; Zhu, Z.-J.; Yan, B.; Bunz, U.H.F.; Rotello, V.M. Colorimetric Bacteria Sensing Using a Supramolecular Enzyme–Nanoparticle Biosensor. *J Am Chem Soc* **2011**, *133*, 9650–9653, doi:10.1021/ja2021729.